

# Efficiency pedestal in quasi-phase-matching devices with random duty-cycle errors

J. S. Pelc,\* C. R. Phillips, D. Chang, C. Langrock, and M. M. Fejer

*E. L. Ginzton Laboratory, Stanford University, 348 Via Pueblo Mall, Stanford, California 94305, USA*

*\*Corresponding author: jpelc@stanford.edu*

Received November 23, 2010; accepted January 17, 2011;

posted February 3, 2011 (Doc. ID 138661); published March 9, 2011

It is shown that random duty-cycle errors in quasi-phase-matching (QPM) nonlinear optical devices enhance the efficiency of processes far from the QPM peak. An analytical theory is shown to agree well with numerical solutions of second-harmonic generation (SHG) in disordered QPM gratings. The measured efficiency of 1550 nm band SHG in a periodically poled lithium niobate (PPLN) waveguide away from the QPM peak agrees with observations of domain disorder in a PPLN wafer by Zygo interferometry. If suppression of parasitic nonlinear interactions is important in a specific application of QPM devices, control of random duty-cycle errors is critical. © 2011 Optical Society of America

OCIS codes: 190.2620, 190.4360.

Quasi-phase-matching (QPM) is a technique by which the phase mismatch between interacting waves in a  $\chi^{(2)}$  frequency conversion process is compensated by a periodic sign flip of the nonlinear coefficient. Although it was one of the first methods considered to achieve unidirectional power flow in three-wave mixing processes [1], it was not until the advent of electric-field periodic poling [2] that quasi-phase-matching came into widespread use in systems as diverse as optical parametric oscillators [3] and ultrasensitive upconverters [4].

QPM gratings are subject to a wide variety of fabrication errors, which can influence the nonlinear optical performance of a device. In this Letter, we extend the earlier analysis of [5] and [6] and show that grating disorder enhances the efficiency of nonlinear interactions away from the QPM peak relative to an ideal grating. Unless the grating disorder can be controlled, the impact of parasitic QPM interactions must be carefully considered for any application of QPM gratings. For instance, in devices for frequency conversion of quantum states of light [4], QPM disorder enhances parametric fluorescence, generating noise photons that degrade the fidelity of quantum-state frequency translation [7]. Below, we present the results of a statistical calculation of the phase-matching behavior of a QPM grating with disorder. We present a measurement of the phase-matching behavior of a periodically poled lithium niobate (PPLN) waveguide, which exhibits an efficiency pedestal that is consistent with that expected from direct measurement of the disorder in the domain duty cycle.

Following [5], we consider second-harmonic generation (SHG) in the limit of low conversion efficiency. In the following, the subscript 1 indicates the fundamental frequency (FF), and 2 indicates the second harmonic (SH). In an ideal first-order QPM grating, the intrinsic wave-vector mismatch  $\Delta k' = k_2 - 2k_1$  is compensated by a periodic reversal in the sign of the nonlinear coefficient  $d(z)$  every coherence length  $l_c = \pi/\Delta k'$ . For a device of length  $L$ , the SH field at  $z = L$  relative to a device with an ideal first-order QPM grating is

$$a_2(L) = \int_0^L g(z) e^{i\Delta k' z} dz, \quad (1)$$

where we have introduced the normalization  $g(z) = (\pi/2L)d(z)/d_0$  such that the Fourier transform  $\tilde{g}(\Delta k')$  represents the SHG relative to an ideal QPM grating.

For a QPM grating with random duty-cycle (RDC) errors, we can write  $g(z)$  as follows:

$$g(z) = \frac{\pi}{2L} \sum_{n=1}^N (-1)^n \Pi\left(\frac{z - (z_n - l_n/2)}{l_n}\right), \quad (2)$$

where  $\Pi((z - z_n)/l_n)$  is a shifted and scaled rectangle function that takes the value 1 for  $|z - z_n|/l_n < 1/2$  and is 0 everywhere else. The relevant quantities relating to RDC errors are illustrated schematically in Fig. 1. We identify  $z_n$  as the position of the  $n$ th QPM domain boundary, and  $l_n = z_{n+1} - z_n$  as the width of the  $n$ th domain. We are interested in the quantity  $\langle |\tilde{g}(\Delta k')|^2 \rangle$ , the efficiency relative to an ideal grating of SHG at a phase mismatch  $\Delta k'$ , where the expectation value is over an ensemble of gratings with randomly perturbed  $z_n$ . To calculate this quantity, we assume  $\langle \delta l_n \rangle$  are independent of the domain number  $n$ , corresponding to preserved long-range order in the grating inherent in production via lithographic processes. We also assert that the domain length errors  $\langle \delta l_n \rangle$  obey Gaussian statistics and define the variance as  $\sigma_l^2$ . For deviations from the QPM peak small compared to an inverse domain length,  $\Delta k = \Delta k' - \pi/l \ll l^{-1}$ , where  $l = \langle l_n \rangle = \Lambda_G/2$ , we find

$$\langle |\tilde{g}(\Delta k)|^2 \rangle = f(\sigma_l) \text{sinc}^2\left(\frac{\Delta k L}{2}\right) + \frac{1 - f(\sigma_l)}{N}, \quad (3)$$

where the function  $f(\sigma_l) = \exp(-\pi^2 \sigma_l^2 / 2l^2)$ .

The normalized SHG efficiency  $\langle |\tilde{g}(\Delta k)|^2 \rangle$  calculated in Eq. (3) consists of two components. The first represents

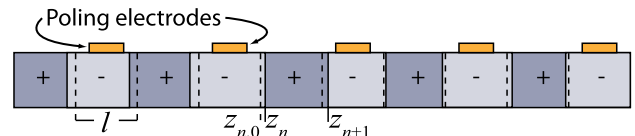


Fig. 1. (Color online) Schematic of RDC errors in a nonideal QPM grating:  $\langle \delta l_n \rangle = 0$ , where  $\delta l_n = l_n - l$ , with  $l_n = z_{n+1} - z_n$  and  $l = \langle l_n \rangle = \Lambda_G/2$ .

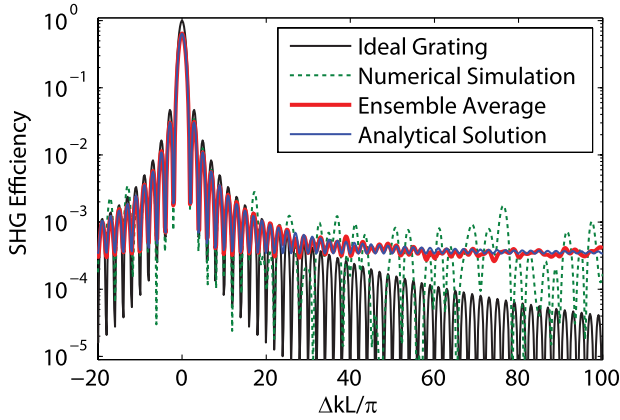


Fig. 2. (Color online) SHG efficiency in a disordered QPM grating versus normalized deviation from the QPM peak; the ensemble average is computed over 100 randomly perturbed gratings, with  $\sigma_l/l = 20\%$ .

the  $\text{sinc}^2(\Delta kL/2)$  tuning behavior of a QPM device with an efficiency reduced by the amount  $f(\sigma_l)$ , an effect discussed in [5]. The second component is a flat QPM pedestal of height  $(1 - f(\sigma_l))/N$  that is independent of  $\Delta k$ . We note that as the grating disorder  $\sigma_l$  is reduced,  $f(\sigma_l)$  approaches 1, and the device regains the characteristics of an ideal grating. Conversely, as the grating disorder is increased, one encounters the behavior of the random QPM devices studied in [6,8], in which the growth of the SH field scales as  $L^{1/2}$ , i.e., the field grows in a random-walk fashion.

To test the analytical theory, we performed both numerical simulations and experiments. Numerically, we constructed an ensemble of 100 disordered QPM gratings, with domain lengths drawn from a Gaussian distribution and with normalized pseudorandom duty-cycle error  $\bar{\sigma}_l = \sigma_l/l = 20\%$ . The SHG tuning behavior for each ideal grating is normalized to the performance of an ideal grating, and an ensemble average is computed. This ensemble average is plotted in Fig. 2 (thick solid red) along with the prediction of the analytical theory (thin solid blue), showing excellent agreement on the height of the QPM pedestal. As one deviates far from the QPM peak, the pedestal predicts elevated generation efficiency when compared with the results for an ideal

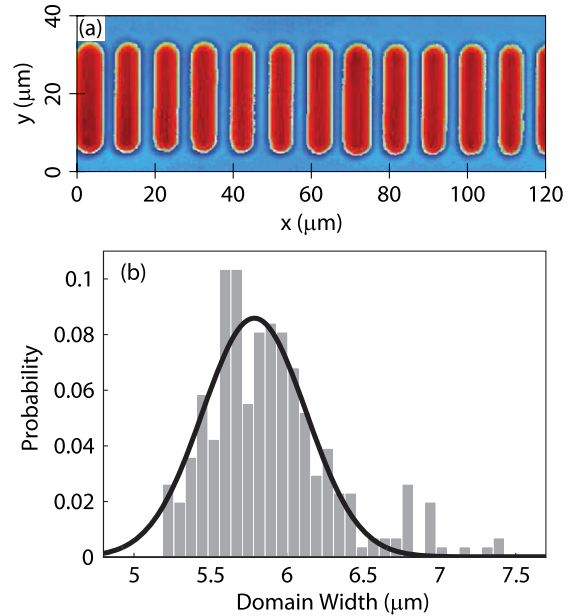


Fig. 3. (Color online) (a) Surface topography of etched PPLN with  $\Lambda_G = 10.22 \mu\text{m}$  measured with a Zygo interferometer, (b) width histogram of approximately 280 inverted domains (bars) and Gaussian fit (black).

QPM grating (thin solid black). Also shown are the results for a single disordered QPM grating (dashed green). We note that while the ensemble average of the pedestal is white, an individual grating can exhibit large fluctuations in efficiency far from the QPM peak.

A direct study of RDC errors via microscopy would enable an estimate of the expected pedestal height in real devices. We fabricated a PPLN wafer by a standard electric-field poling process [3] and etched the original  $+z$  surface to provide topographic contrast between the two domain orientations. The surface topography was imaged using a Zygo microscope; a portion of a typical image is shown in Fig. 3(a). Images were collected along the grating spanning the whole 3 in. wafer, and the domain widths were calculated from the images. A histogram of the inverted domain sizes is shown in Fig. 3(b), showing a mean domain width for the inverted domains of

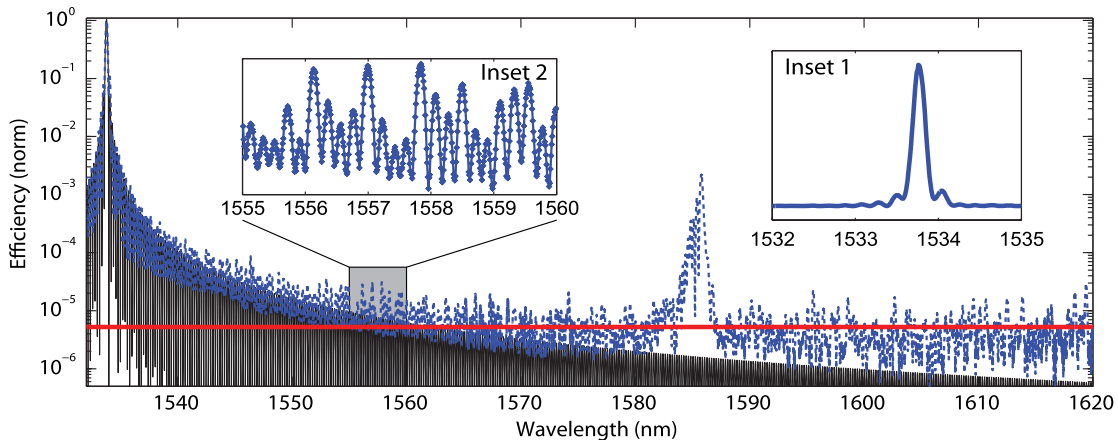


Fig. 4. (Color online) Measured relative SHG efficiency  $\langle |g(\lambda)|^2 \rangle$  (blue dashed) plotted against  $\text{sinc}^2(\Delta kL/2)$  QPM tuning curve (solid black), showing the efficiency pedestal far from the QPM peak. Inset 1, measured SHG tuning curve plotted on linear scale; Inset 2, zoom of measured data between 1555 and 1560 nm.

5.90  $\mu\text{m}$ , which for the poling period  $L_G = 10.22 \mu\text{m}$  corresponds to a mean duty cycle of 58%. We calculate  $\sigma_l = 0.41 \mu\text{m}$ , which corresponds to normalized RDC error of  $\bar{\sigma}_l = 8.0\%$ . The solid curve in Fig. 3 is a fit to a Gaussian distribution, which shows good agreement with the observed histogram, supporting the assumptions made in the development of the analytical theory. The only significant deviation from Gaussian statistics is a longer tail toward larger domains, but SHG simulations with domain statistics drawn from the Zygo measurements agreed within 2% to simulations with domain statistics drawn from a Gaussian distribution with the measured mean duty cycle and variance.

We also studied the phase-matching behavior of SHG in a real QPM device with RDC errors. Because the theory and simulations both describe plane-wave physics, we performed experiments using guided-wave interactions, which are mathematically isomorphic to plane-wave interactions. We fabricated reverse-proton-exchanged PPLN waveguide devices with 59-mm-long QPM gratings. The waveguides incorporate mode filters and adiabatic tapers to facilitate launching the FF fundamental spatial mode [4]. The output facet of the waveguide was polished at an angle of  $5^\circ$  to prevent Fabry–Perot interference effects. The poling period was 15.9  $\mu\text{m}$ , which resulted in a first-order QPM peak at 1533.75 nm at a temperature of 25  $^\circ\text{C}$ , as seen in Inset 1 of Fig. 4. In the experiment, we used two external cavity diode lasers to cover the 90 nm measurement range. The FF light was modulated with a mechanical chopper and was coupled in and out of the waveguide using aspheric lenses ( $f = 8 \text{ mm}$ ), and the outgoing SH and residual FF light were separated using a dichroic mirror. The SH light was detected using an unbiased Si photodiode and a lock-in amplifier at the chopper frequency, and the outgoing FF light was monitored using a calibrated InGaAs detector. The FF wavelength was stepped in increments of 0.01 nm, and the sensitivity of the lock-in amplifier was adjusted depending on the SH signal level to enable a high dynamic range measurement.

The normalized SHG efficiency  $\langle |\tilde{g}(\lambda)|^2 \rangle$  was computed from the measured SH and FF data and is plotted as the dashed curve in Fig. 4. When compared with the phase-matching behavior of an ideal grating (solid black curve), at large detunings from the QPM peak one observes a QPM pedestal. Although the data appear noisy, ripples in the generation efficiency are in fact well resolved by the lock-in measurement technique, as demonstrated by Inset 2, which shows an expansion of the data from 1555 to 1560 nm. Similar ripples are observed in the simulations, and the observed spectral features are repeatable from measurement to measurement. The solid red line is the average efficiency far from phase matching; the pedestal height  $\langle |\tilde{g}(\lambda)|^2 \rangle = 5.2 \times 10^{-6}$ , which corresponds

to an RDC error of  $\bar{\sigma}_l = 8.9\%$ . The small peak at 1586 nm has a height 27 dB below the QPM peak and is due to an interaction involving a higher-order spatial mode of the waveguide. Because of an imperfect mode filter and/or adiabatic taper at the input of the waveguide, there is residual coupling to the  $\text{TM}_{01}$  mode of the waveguide at the FF. Modal field simulations [9] predict that for a QPM peak at 1534 nm, one also expects a first-order QPM peak for the SFG interaction between the  $\text{TM}_{00}$  and  $\text{TM}_{01}$  modes at an FF corresponding to 1586 nm.

Random duty-cycle errors are inherent in the fabrication of periodically poled materials via lithographic methods. Early analysis of QPM devices showed that RDC errors reduce the peak efficiency of a device [5]. Here we have demonstrated, using a combination of analytical calculations, simulations, and SHG experiments, that RDC errors also result in a QPM pedestal, which enhances the efficiency of processes far from the QPM peak. We have directly observed the RDC errors via optical imaging of an etched PPLN sample; the observed value  $\bar{\sigma}_l = 8.0\%$  is consistent with the pedestal height observed in the SHG experiment. If suppression of parasitic interactions is an important consideration for a particular application of QPM devices, the control of RDC errors is critical.

J. S. Pelc was supported by a Robert N. Noyce Stanford Graduate Fellowship. Additional support is provided by the Air Force Office of Scientific Research (AFOSR) under grant FA9550-09-1-0233 and Army Research Office (ARO) under grant DAAD19-03-1-0199. The authors thank I. W. Jung for assistance with the Zygo measurement.

## References

1. J. A. Armstrong, N. Bloembergen, J. Ducuing, and P. S. Pershan, *Phys. Rev.* **127**, 1918 (1962).
2. M. Yamada, N. Nada, M. Saitoh, and K. Watanabe, *Appl. Phys. Lett.* **62**, 435 (1993).
3. L. E. Myers, R. C. Eckardt, M. M. Fejer, R. L. Byer, W. R. Bosenberg, and J. W. Pierce, *J. Opt. Soc. Am.* **12**, 2102 (1995).
4. C. Langrock, E. Diamanti, R. V. Roussev, Y. Yamamoto, M. M. Fejer, and H. Takesue, *Opt. Lett.* **30**, 1725 (2005).
5. M. M. Fejer, G. A. Magel, D. H. Jundt, and R. L. Byer, *IEEE J. Quantum Electron.* **28**, 2631 (1992).
6. S. Helmfrid and G. Arvidsson, *J. Opt. Soc. Am. B* **8**, 797 (1991).
7. J. S. Pelc, C. Langrock, Q. Zhang, and M. M. Fejer, *Opt. Lett.* **35**, 2804 (2010).
8. M. Baudrier-Raybaut, R. Haïdar, Ph. Kupecek, Ph. Lemasson, and E. Rosencher, *Nature* **432**, 374 (2004).
9. R. V. Roussev, "Optical-frequency mixers in periodically poled lithium niobate: materials, modeling, and characterization," Ph.D. dissertation (Stanford University, 2006).